



0038-1098(95)00561-7

QUANTITATIVE DETERMINATION OF HEXAGONAL MINORITY PHASE IN CUBIC GaN USING
RAMAN SPECTROSCOPY

H. Siegle, L. Eckey, A. Hoffmann, and C. Thomsen

Institut für Festkörperphysik, Technische Universität Berlin, 10623 Berlin, Germany

B. K. Meyer

Physikdepartment E16, Technische Universität München, 85747 München, Germany

D. Schikora, M. Hankeln, and K. Lischka

Institut für Optoelektronik, Universität Paderborn, 33095 Paderborn, Germany

(Received 19 July 1995; accepted 10 August 1995 by M. Cardona)

We show that Raman scattering is a very sensitive and straightforward tool for the quantitative determination of a structural minority phase in GaN. In- and on-plane excitations, as well as polarization dependent measurements on predominantly cubic and hexagonal GaN samples, were performed and forward scattering effects were found. We were able to verify as an example the phase purity of a cubic GaN sample down to the 1% level.

Keywords: A. semiconductors, C. crystal structure and symmetry, D. phonons, E. inelastic light scattering, E. luminescence

GaN has received considerable attention over the last years as a promising material for applications in optoelectronics in the blue and ultraviolet spectral range [1]. In the past, extensive investigations have been performed on samples with wurtzite crystal structure, but more recently some groups were able to prepare zincblende-structure layers on various substrates [2,3,4]. A major difficulty in the growth of cubic GaN is the polytypism of this material. During the growth process subdomains of hexagonal phases may be built in via a stacking fault mechanism [5]. Using off-axis x-ray diffractometry Lei et al. [6] and Brandt et al. [7] showed that cubic domains existed in their predominantly hexagonal GaN and vice versa. In contrast to this,

standard θ - 2θ x-ray scans frequently used to demonstrate the crystal quality of grown samples are unable to determine a possible minority phase present in a sample. If the c-axis, e.g., in hexagonal subdomains is tilted by a few degrees with respect to the cubic majority phase only Bragg peaks originating from the majority phase are observable. Therefore, θ - 2θ scans are less suitable for obtaining information about a possible minority-phase content.

Regardless of the particular advantages that one of the two crystal structures of GaN may have over the other, it is important to unambiguously distinguish the two phases when comparing experimental results. We

show here with the example of the near-gap luminescence of GaN that it is valuable to know the phase purity of the structures investigated. In both a cubic and a hexagonal sample we found similar luminescence peaks, and in order to make statements specific to one phase it is important to be sure that the luminescence does not originate from minority phase domains. We show that Raman spectroscopy is able to verify the purity of GaN layers with respect to polytype-domain formation. The different polarisation scattering selection rules allow us to distinguish the two phases by selecting appropriate scattering geometries and put us in the position to determine the hexagonal-phase content in a nominally cubic sample down to the 1% level.

The GaN films investigated here were grown using MBE and MOCVD. A $0.6\mu\text{m}$ thick layer was grown on (001) GaAs by MBE. The stoichiometry of the growing GaN-layer was adjusted by RHEED-measurements of the surface reconstruction. The growth of the cubic phase was performed using Ga-rich conditions. Reflection x-ray diffraction spectra taken from this sample in conventional θ - 2θ geometry show only cubic diffraction peaks indicating that the plane perpendicular to the x-ray scan did not contain hexagonal GaN lattice planes. A typical MOCVD $2\mu\text{m}$ thick wurtzite layer grown on sapphire served as hexagonal reference. Raman-scattering experiments (resolution 2 cm^{-1}) were excited with the 632.8 nm line of a HeNe laser. The scattered light was detected in backscattering geometry and analyzed by a Dilor LABRAM single-grating spectrometer with a charge-coupled device (CCD) detector.

The low-temperature photoluminescence spectra of the hexagonal and the cubic GaN sample after excitation at 3.75 eV are compared in Fig. 1. The spectrum of the hexagonal sample is dominated by the donor-bound exciton line appearing at 3.472 eV [8]. Two further lines are observed at 3.360 eV and 3.307 eV. The broad and very weak structure at 3.27 eV is due to

donor-acceptor-pair transitions as shown by time-resolved photoluminescence [9]. The lower spectrum of the cubic sample resembles that of the hexagonal sample in its lower-energy features. Except for an energy shift of 5 meV, which can be explained by a different strain in the two samples, the two dominating lines of the cubic sample, at 3.365 eV and 3.312 eV, exhibit the same energy difference, spectral appearance, and almost the same intensity ratio as the corresponding lines of the hexagonal sample. The weak lines appearing at 3.285 eV and 3.293 eV in the lower spectrum cannot be resolved in the hexagonal sample because of the spectral overlap with the donor-acceptor-pair transitions. They have been observed, however, in other hexagonal samples not showing the donor-acceptor-pair band. A very weak line from the cubic sample is observed at 3.44 eV.

Summarizing the PL results, we find nearly identical luminescence features in both hexagonal and cubic GaN. There exists thus the possibility, that the origin of the luminescence is the same in both samples; the nominally cubic sample may contain, e.g., subdomains of hexagonal GaN which may have remained

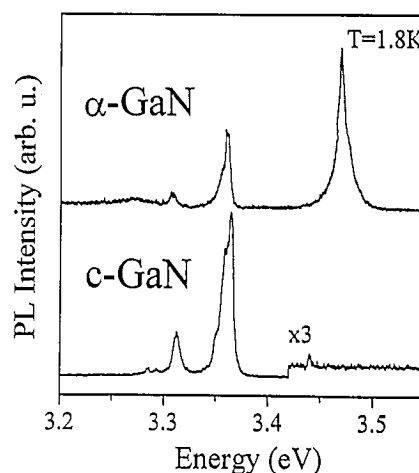


FIG. 1: Low-temperature photoluminescence spectra of the hexagonal and cubic sample after excitation at 3.75 eV.

undetected by x-ray scattering. For this purpose, we have performed the Raman measurements described in the following.

We consider here primarily the possibility that there is a hexagonal minority phase in cubic GaN. There are two principally different possibilities for the orientation of hexagonal subdomains in cubic GaN. In the first case, the c-axis [0001] of the hexagonal phase of GaN is tilted only by a few degrees with respect to the c-axis of the otherwise cubic material. In the second case the [0001] axis is parallel to a cubic $\langle 111 \rangle$ direction, i.e., the space diagonal of the cubic unit cell; the second case occurs as a result of the stacking fault mechanism [5].

We discuss now first the case of small angles between the c-axis of a supposed hexagonal minority phase and the cubic film, where standard θ - 2θ x-ray scans are unable to detect the hexagonal material. In

contrast to the coherent process of x-rays, where the scattering intensity is obtained by first adding and then squaring, the Raman intensity is the sum of the squared amplitudes [10]. Therefore, small deviations from principal angles do not affect the Raman-scattering intensity significantly, and the minority-phase orientation can be considered as approximately parallel to the cubic phase.

Cubic GaN has zincblende structure and belongs to the point group $T_d=43m$. Zincblende-type materials have close to $k=0$ a doubly degenerate TO and a single LO phonon with a higher frequency. Hexagonal GaN grows in wurtzite structure and belongs to the space group $C_{6v}=6mm$. One A_1 , one E_1 , and two E_2 modes out of eight sets of modes predicted by group theory are Raman active [11]. The wurtzite material may be considered as having a slightly distorted zincblende structure with a small change in nearest neighbor

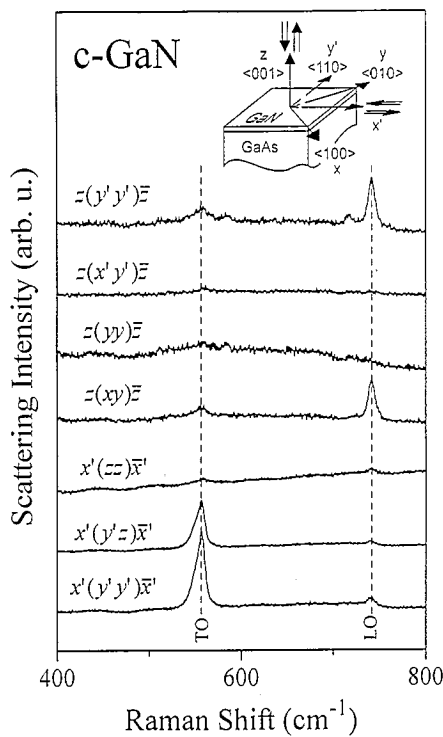


FIG. 2a: Room-temperature Raman spectra taken from the cubic sample in various configurations. The inset shows the corresponding scattering geometries.

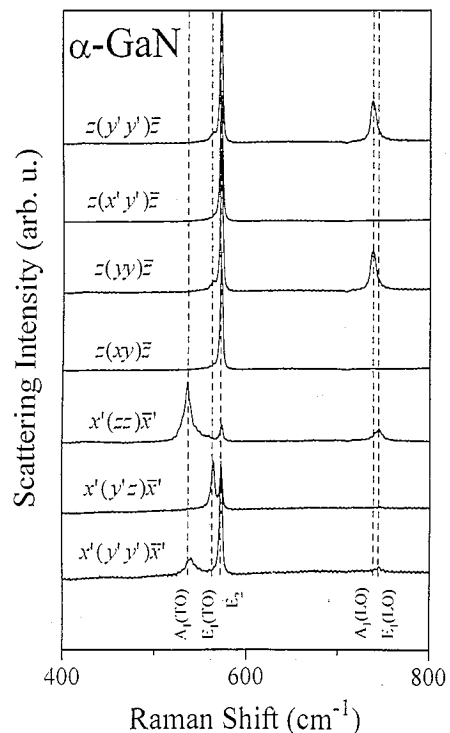


FIG. 2b: Room-temperature Raman spectra taken from the hexagonal sample in various configurations.

Tab. 1: Phonon frequencies in hexagonal and cubic GaN obtained by Raman spectroscopy at room temperature.

Hexagonal Modes	A ₁ (TO)	E ₁ (TO)	E ₂	A ₁ (LO)	E ₁ (LO)
Frequency (cm ⁻¹)	533	561	570	735	742
Cubic Modes	TO		LO		
Frequency (cm ⁻¹)	555		740		

distance; consequently the energy difference between the Raman modes of hexagonal and cubic GaN is not very large.

Figure 2a and Fig. 2b show room-temperature Raman spectra of cubic and hexagonal GaN in various configurations, respectively. The frequencies of all the modes observed are listed in Tab. 1 and agree well with the results of other workers [12-14].

The small energy difference between the modes of the two modifications of GaN makes it difficult to determine the minority-phase content. Especially in backscattering geometry where the incoming and

scattered light vector are parallel to the c-axis, $z(\cdot)\bar{z}$, a frequently used arrangement, both the two cubic (LO, TO) and the two hexagonal modes (E₂, A₁(LO)) appear at nearly the same frequency. In order to distinguish the cubic and the hexagonal phase we have taken advantage of the different point groups of the two polytypes of GaN leading to different selection rules for first-order Raman scattering.

The Raman tensors for T_d and C_{6v} [11] lead to the selection rules for the two surfaces (001) and (110) considered here (Tab. 2). In the last column the allowed modes of hexagonal GaN are listed provided that the [0001] axis is parallel to incident and scattered wave

Tab. 2: Raman selection rules for backscattering configurations used in this work (the c-axis of the cubic GaN is parallel to the z direction). The selection rules are only weakly relaxed if the angle between the [0001] axis and *k* is small.

Surface	Incident Polarization	Scattered Polarization	Porto Notation	Allowed Modes	
				Cubic	Hexagonal
[001]	[110]	[110]	$z(y'y')\bar{z}$	LO	E ₂ , A ₁ (LO)
	[110]	[110]	$z(x'y')\bar{z}$	-	E ₂
	[100]	[100]	$z(yy)\bar{z}$	-	E ₂ , A ₁ (LO)
	[010]	[100]	$z(xy)\bar{z}$	LO	E ₂
[110]	[001]	[001]	$x'(zz)\bar{x}'$	-	A ₁ (TO)
	[110]	[001]	$x'(y'z)\bar{x}'$	TO	E ₁ (TO)
	[110]	[110]	$x'(y'y')\bar{x}'$	TO	A ₁ (TO), E ₂

vectors. A diagram of the corresponding scattering geometries is shown in the inset of Fig. 2a.

Comparing Tab. 2 with the corresponding Raman spectra shows that the selection rules were well satisfied, except for the E_2 mode weakly visible in the $x'(zz)\bar{x}'$ and $x'(y'z)\bar{x}'$ configurations. The $E_1(\text{LO})$ mode appears in the $x'(zz)\bar{x}'$ configuration due to Fröhlich interaction [10]. As can be seen from Tab. 2 it is possible to distinguish the two phases of GaN using the $z(\dots)\bar{z}$ configuration because of the different selection rules of the cubic LO and the hexagonal $A_1(\text{LO})$ mode in spite of their closeness in frequency. While in $z(y'y')\bar{z}$ configuration both modes are observable, in the configuration rotated by 45° in the polarization plane, $z(yy)\bar{z}$, only the hexagonal $A_1(\text{LO})$ mode is allowed. It is clear that the two phases can only be distinguished using these configurations if the sample is grown epitaxially. If the cubic GaN layer is oriented only in growth direction but not perpendicular to it there are obviously no selection rules involving x- and y-polarizations. The difference in the $z(y'y')\bar{z}$ and $z(yy)\bar{z}$ spectra in Fig. 2a obtained on the cubic sample shows its phase purity. In order to estimate the *cubicity* quantitatively we fitted a Lorentzian to the allowed polarization ($y'y'$) and compared it to the spectrum in yy -polarization. We can estimate the hexagonal fraction present in this spectrum to be less than 2% (having corrected for the different thicknesses and relative Raman coefficients). Thus, less than 2% hexagonal subdomains were built in to our cubic sample.

It is interesting to note that the weak structure at 560 cm^{-1} in the $z(y'y')\bar{z}$ spectrum in Fig. 2a does not originate from a hexagonal minority phase although that would be possible from a polarization point-of-view (Tab. 2). The opposite is the case: this structure belongs to a TO mode of the cubic phase and appears in these spectra because of forward scattering which, to our knowledge, has not been mentioned in previous publications on Raman scattering on cubic GaN. Forward scattering occurs in this case because the

exciting laser is reflected from the interface between the transparent layer and the substrate. The reflected light contributes to the total Raman excitation where, in contrast to backscattering, the k transfer is perpendicular to the normal of the film [001], i.e., it takes place in the xy-plane. The Raman-tensor symmetry for forward scattering of TO phonons is the same as for LO phonons in backscattering geometry. Forward scattering is allowed in the configuration $z(y'y')\bar{z}$ and $z(x'y')\bar{z}$, and we can see the corresponding weak structure in the figure. We can prove this point in a configuration in which the corresponding hexagonal mode is allowed and the cubic modes are forbidden as is the case for $z(yy)\bar{z}$ (Fig. 2a). Only a background originating from second-order scattering the GaAs substrate is visible in the trace. Thus, the structures observed at 560 cm^{-1} in $z(y'y')\bar{z}$ and $z(x'y')\bar{z}$ in Fig. 2a are caused by forward scattering of TO phonons and not by a minority hexagonal phase.

To determine the phase purity of a GaN samples using $z(\dots)\bar{z}$ configurations one has thus to be sure that the investigated layer was grown epitaxially, and attention has to be paid to forward-scattering effects. A desirable unambiguous method for the quantitative determination of the cubicity is obtained for Raman

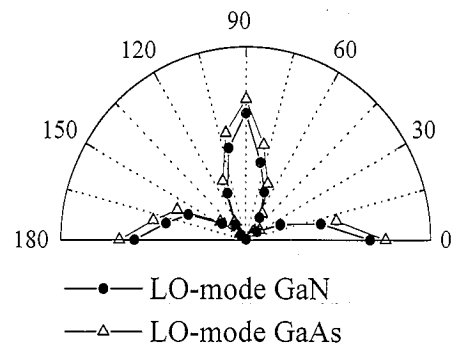


FIG. 3: Polarization dependence of the parallel polarized GaN and GaAs LO-phonon intensity as the sample is rotated. An angle of 45° corresponds to $z(yy)\bar{z}$.

excitation in the plane of the substrate (Fig. 2b). From the $x'(zz)\bar{x}'$ or $x'(y'y')\bar{x}'$ configuration the hexagonal phase content can easily be determined. The $E_1(\text{TO})$ mode which appears nearly at the same frequency as the cubic TO mode is forbidden in the $x'(y'y')\bar{x}'$ configuration (Tab. 2). Therefore, comparing the intensity ratio of the cubic mode to the allowed hexagonal E_2 mode it is possible to determine the minority hexagonal phase content quantitatively. Using the same fit procedure described above we obtain for the cubic sample investigated in this paper a cubicity of $99\pm 1\%$. Thus, both, on- and in-plane excitation lead in case of small angles between the cubic and hexagonal phase to the result that the hexagonal phase is nearly absent in this sample.

We come now to the second principally different way a hexagonal domain may be built in in an otherwise cubic material. Lei et al. [6] and Brandt et al. [7] showed using off-axis x-ray diffraction that minor hexagonal parts of GaN preferred to be built in such a way that the [0001] direction was parallel to a $\langle 111 \rangle$ direction of the cubic basic material. As before, standard θ - 2θ scans are unable to detect hexagonal subdomains. Raman experiments, however, lead in all configurations possible here to a signal from the hexagonal phase.

In order to obtain quantitative information we measured the polarization dependence of the phonon modes of the cubic sample. Fig. 3 shows polar plots of the intensity of the LO phonon mode of GaN compared to the LO mode of GaAs. In this experiment the incident and scattered polarizations were kept fixed and parallel polarized, while the sample was rotated in total by 180° in the plane defined by the polarizations. The GaN mode shows the same polarization dependence as the GaAs mode indicating that the sample is grown epitaxially. If both phases coexisted in the sample, the different polarization dependences would overlap and the distinct d-wave like minima of the scattering intensity would

disappear with increasing hexagonal-phase content. From these considerations we found a cubicity of $98\pm 2\%$. Thus, the cubic sample investigated contains at most 2% hexagonal subdomains.

In conclusion we have shown in this paper that Raman scattering is a very sensitive and straightforward suitable tool for determining a structural minority phase in GaN quantitatively. We were able to verify as an example the phase purity of a cubic GaN sample down to the 1% level. Since this cubic sample exhibits a very similar photoluminescence as a predominantly hexagonal sample the intrinsic luminescence of Fig. 1 is either the same for cubic and hexagonal GaN or hexagonal subdomains, with a volume fraction of smaller than 1%, are at the origin of the luminescence also in nominally cubic GaN. Alternatively, the interface region could be responsible for the luminescence in both cubic and hexagonal GaN. For the analysis of structural subdomains we distinguished two cases. In the case of small angles between the c-axes of the two phases of GaN we found that hexagonal subdomains may be determined comparing the $z(y'y')\bar{z}$ and $z(yy)\bar{z}$ spectra under the assumption that the investigated film is grown epitaxially and under consideration of the forward-scattering contribution. We have shown that an in-plane excitation using $x'(zz)\bar{x}'$ or $x'(y'y')\bar{x}'$ configurations is more precise allowing for an error down to the 1% level. In the case of large angles between the two c-axes we measured the polarization dependence of the cubic LO phonon in order to determine accurately the cubicity. In this case we were able to prove the phase purity of our sample down to a 2% level. Raman scattering thus allows the determination of structural subdomains in nominally purely hexagonal or cubic GaN to a high accuracy without the possible pitfalls of conventional θ - 2θ x-ray scans.

References

- [1] R. F. Davis, IEEE **79**, 702 (1991); S. Strite and H. Morkoç, J. Vac. Sci. Technol. **B10**, 1237 (1992)
- [2] M. Mizuta, S. Fujieda, Y. Matsumoto and T. Kawamura, Jap. J. Appl. Phys. **25**, L945 (1986)
- [3] M. J. Paisley, Z. Sitar, J. B. Posthill and R. F. Davis, J. Vac. Sci. Technol. **A7**, 701 (1989)
- [4] T. Lei, M. Fanciulli, R. J. Molnar, T. D. Moustakas, R. J. Graham and J. Scanlon, Appl. Phys. Lett. **59**, 944 (1991)
- [5] S. Strite, M. E. Lin and H. Morkoç, Thin Solid Films **231**, 197 (1993)
- [6] T. Lei, K. F. Ludwig, T. D. Moustakas, J. Appl. Phys. **74**, 4430 (1993)
- [7] O. Brandt, H. Yang, B. Jenichen, Y. Suzuki, L. Däweritz, and K. H. Ploog, to be published
- [8] R. Dingle, D. D. Sell, S. E. Stokowski, and M. Ilegems, Phys. Rev. B **4**, 1211 (1971)
- [9] R. Dingle and M. Ilegems, Solid State Comm. **9**, 175 (1971)
- [10] M. Cardona, in: Light Scattering in Solids II, ed. by M. Cardona and G. Güntherodt, Topics Appl. Phys. **50** (Springer, Berlin, Heidelberg 1982), p. 19ff
- [11] C. Thomsen, R. Wegerer, H.-U. Habermeier, and M. Cardona, Solid State Comm. **83**, 199 (1992)
- [12] T. Kozawa, T. Kachi, H. Kano, Y. Taga, and M. Hashimoto, J. Appl. Phys. **75**, 1098 (1994)
- [13] S. W. Brown, S. C. Rand, C.-H. Hong, and D. Pavlidis, Mat. Res. Soc. Symp. Proc. **339**, 503 (1994)
- [14] S. Miyoshi, K. Onabe, N. Ohkouchi, H. Yaguchi, R. Ito, S. Fukatsu, and Y. Shiraki, J. Crystal Growth **124**, 439 (1992)